Wavelength Dependence of Optical Electronic Nose for Ripeness Detection of Oil Palm Fresh Fruits

Ikhsan Rahman Husein, Minarni Shiddiq*, Dewi Laila Sari, Annisa Putri

Department of Physics, Universitas Riau, Indonesia

ABSTRACT

Electronic noses have been developed as an artificial sense to imitate the human nose based on volatile gases. They have been used in agriculture to monitor and predict fruit qualities such as ripeness and chemical contents. Electronic noses with semiconductor gas sensors have a limitation of volatile gases detected. Therefore, optical electronic noses using an output coupler become an alternative due to the wavelength dependency of the gas types. The ripeness of oil palm fresh fruit bunches (FFBs) is one of the main factors in determining the quality of crude palm oil. Electronic detection is preferable to substitute the manual methods for ripeness detection. This study built an optical electronic nose and analyzed the wavelength dependence on the detection performance. The electronic nose consisted of an infrared LED and a photodiode enclosed in a chamber, a microcontroller, and a sample chamber. We tested four infrared LEDs with 760, 780, 840, and 910 nm wavelengths. The samples were fruitlets taken from oil palm FFBs, previously categorized as unripe, ripe, and overripe. The fruits were grounded, inserted into the sample chamber, and preheated to increase the volatile gas concentration. Trapezoid areas represented the time-varying output voltages for each LED. The results showed that overripe fruits had slightly higher trapezoid areas. LED of 840 nm wavelength obtained higher trapezoid areas. LED of 780 nm was the best candidate for the electronic nose due to linearity in increasing trapezoid areas. The results showed the potential of the optical electronic nose for oil palm fruits.

ARTICLE INFO

* **Corresponding Author**
E-mail address: minarni.shiddiq@lecturer.unri.ac.id

1. INTRODUCTION

Electronic noses (e-nose) have continuously evolved due to their increasing applications in many fields, especially for evaluating and monitoring the qualities of agricultural and food products. The term e-nose usually describes a device consisting of an array of sensitive gas sensors, conditional and controlling circuits, acquisition and analysis process, and pattern recognition algorithms. The operating principle of an e-nose simulates the function of human olfactory receptors. E-noses play a crucial role in fingerprinting the internal characteristics of fruits or foods due to unique volatile gases emitted, especially during ripening or storing [1, 2]. Applications of e-noses in food industries include bacterial foodborne pathogen detection [3] and microbial contamination diagnosis [4]. In agricultures, e-noses have been used for monitoring fruit quality monitoring and evaluation [5], such as forecasting the days before decay of peach fruit [6]. The other significant e-nose applications were for biomedical purposes, such as monitoring and diagnosing disease [7] and screening the environment by detecting pollutants, hazardous chemicals, and explosives [8].

Electronic noses offer some advantages compared to other odor detection techniques. E-nose has become a quick, no-destructive, and real-time method to substitute traditional gas detections and gas chromatography [9]. Numerous applications of e-nose rely on their ability to produce pattern analysis of gas-phase mixtures consisting of volatile organic compounds (VOCs) and some non-VOCs

such as inorganic gases. VOCs are carbon-based compounds ($C_2 - C_{30}$), which include a diverse group of compounds such as hydrocarbons, esters, alcohols, ketones, and aldehydes with high vapor pressures and low boiling points (50°C – 260°C) [10]. The primary advantages of e-noses are relatively simple systems and operations. The e-nose system has flexibility in designs and purposes that depend on the types of gas sensors and pattern recognition methods.

Electronic noses have used a variety of gas sensors. Gas sensors made of conducting polymers, metal-oxide-semiconductor (MOS), quartz crystal microbalance, and surface acoustic wave sensors have been used for pollutant, hazardous gas detection [9]. These gas sensors work based on the electrical properties of sensor materials. MOS gas sensors are the most widely used for many applications because of their low cost, high stability and precision [11, 12]. However, MOS sensors have limitations on the types of gases detected.

Another type of e-nose that has drawn the attention of researchers is an optical electronic nose. Optical electronic noses use optical gas sensors, which work based on the optical properties of the sensor materials [12]. The optical gas sensors measure optical characteristics of light interaction with VOCs, such as the absorbance of light. One of the advantages of using optical sensors is fewer environmental effects on the optical sensor response since this method is not related to chemical reactions. Other advantages of the optical sensor mechanism are higher sensitivity to various VOCs, good selectivity, especially for gases such as CO_2 and CH_4, good response or recovery time, and longer sensor lifetime than other gas sensors [13, 14]. However, optical sensors have some limitations, such as being more expensive and lower portability [8].Optical e-noses have applications such as detecting total soluble solid contents of orange [15] and monitoring Tilapia fish microbial spoilage [16].

Oil palm fresh fruit bunches (FFBs) are the prime commodity in Indonesia and Malaysia as the sources of crude palm oil (CPO). The properties of FFBs define the CPO qualities. One of the quality factors of FFBs is ripeness levels which affect the oil and free fatty acid (FFA) contents. Unripe FFBs has lower oil and FFA, while overripe FFBs has higher FFA, which should be less than 5%. Many circumstances make the qualities of FFBs arrived at oil palm refinery change. Most sorting and grading processes are done manually and traditionally using trained graders. The traditional method used for FFBs ripeness classification relies on the FFBs surface color change and the number of fruitlets loosed. Maintaining CPO quality and keeping higher efficiency in time, labor shortage and costs need automatic sorting and grading [17].

There have been extensive efforts to automate the sorting and grading process of FFBs for oil palm mills based on ripeness levels. Many methods developed were imaging techniques such as using color cameras or computer vision [18] and thermal imaging [19]. These methods are relatively simple but need expertise in image processing. The other methods were using electronic sensors, such as a pair of LED at 670 nm and phototransistor [20], a 635 nm diode laser and two photodiodes [21]. E-nose system has been used for oil palm plants, such as to detect the Ganoderma infection that causes basal stem rot (BSR) disease [22, 23]. E-nose for oil palm FFBs ripeness detection used MOS sensors such as MQ sensor arrays [24].

Detection of fruit ripeness using an electronic nose is possible since fruits produce VOCs. E-noses are efficient, non-destructive, reliable instruments for grading fruits based on fruit aroma, the substitute for experienced fruits grader [25]. Oil palm FFBs have unique physical, chemical, and optical properties thatare useable for ripeness identification. The fruitlets of FFBs have four parts, exocarp, mesocarp, endocarp, and kernel. Mesocarp and kernel are the sources of palm oil known as CPO and crude palm kernel oil. Mesocarp has higher oil content which increases during ripening. For e-nose purposes, the chemical constituents of palm oil become the marker for fruit ripeness levels. Palm oil contains 50% saturated fatty acids, which have a high proportion of palmitic acid, oleic, and linoleic acids [26]. Using gas chromatography and mass spectrometry have found that crude and oxidized palm oil have VOCs associated with fresh palm oil and nutty aromas.

The optical properties of oil palm fruits are associated with the chemical contents found in the oil palm exocarp and mesocarp layers. The chemical contents are chlorophyll, anthocyanin, flavonoids, carotenoids, and triacylglycerols [27, 28]. The concentrations of chlorophyll and anthocyanin pigments are responsible for the skin color of oil palm fruits, which are higher for unripe and lower for underripe and ripe fruits. The pigments have different absorbance and reflectance wavelengths.

This study developed an optical e-nose system to detect the ripeness levels of the oil palm fruit. The system used a LED-photodiode pair sensor [14], contained in a chamber connected by a hose to the sample chamber. We used four LEDs as the light sources with different wavelengths in the infrared region. The measurement process was controlled using Arduinoand PLX-DAQ. The trapezoidal areas were calculated to represent the time-varying output voltages of the photodiode. The samples were fruitlets detached from oil palm fresh fruit bunches with three ripeness levels, grounded, placed in the sample chamber, and preheated before drawn VOCs gases of the samples to the sensor chamber. The CO_2 gas was used to calibrate the e-nose system. We analyzed the relations of the response time of the sensor to each wavelength dependence, and trapezoidal area to ripeness levels.

2. MATERIALS AND METHOD

2.1. Sample Preparation

In this study, the samples were fruits loosed from nine oil palm FFBs of the Tenera variety. The samples respectively consisted of three unripe, ripe and overripe FFBs, previously categorized by an experienced harvester as shown in Figure 1. Each FFBs has front and back sides. Ten adjacent fruits were taken from the bottom and top part of each side and saved in a labeled plastic bag for further process. The ten fruits were peeled, grounded, mixed with purified water, and put into a sample chamber. The number of samples from each FFBs was 40 fruits from 4 parts.The measurements were carried out three times for each sample.
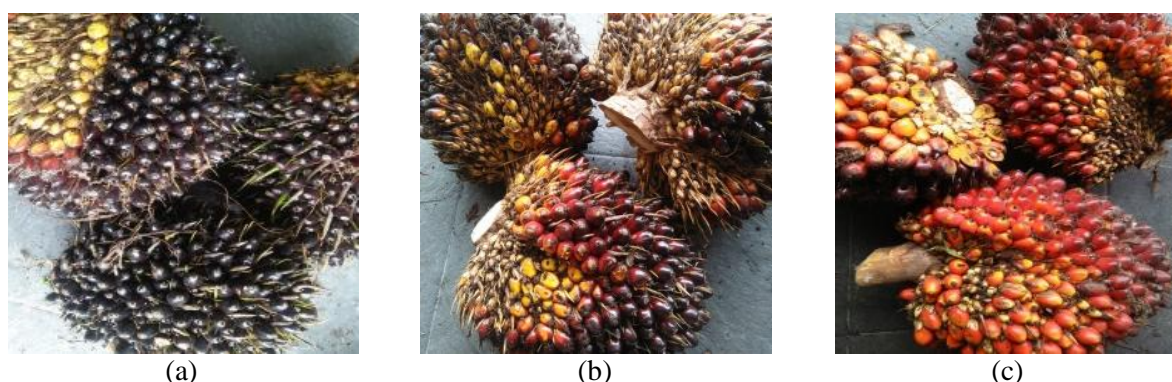

| (a) | (b) | (c) |

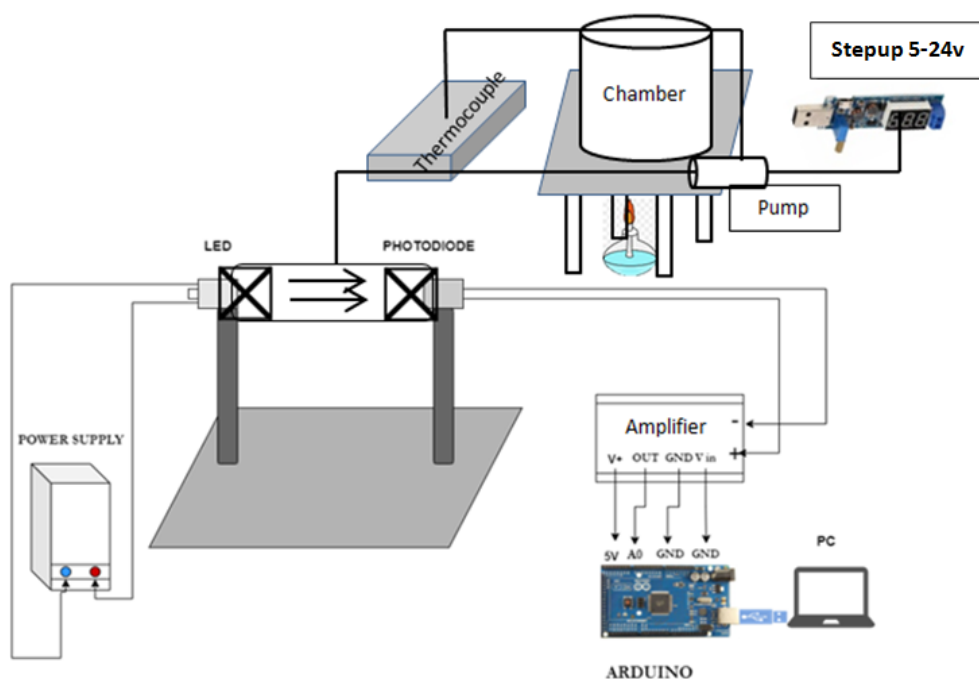**Figure 1.** Palm fruit samples for (a) unripe, (b) ripe, and (c) overripe level.

Figure 2. Optical e-nose systemwith optic and electrical circuit.

Wavelength dependence of optical electronic nose for ... (Ikhsan Rahman Husein)

2.2. Optical Electronic Nose System

The optical e-nose system applied photodiode as a receiver and LED as a transmitter shown in Figure 2. Both components have wavelength sensitivity in the infrared region. We used four LEDs with wavelengths of 760, 780, 840, and 910 nm with bandwidths of 30 – 50 nm [14].

The LED and photodiode pair was enclosed in an acrylic chamber. The chamber had dimension of 3 cm in length and 0.5 cm in radius. On the top of this chamber, there was a hose connecting to the sample chamber to let VOCs gases from the sample chamber flowing between the LED and photodiode.The e-nose system was set on an optical table. The LED was connected to a power supply of 1.5 – 2 V and the photodiode to a trans-impedance amplifier.

The electronic circuits of the system consisted of several components such as Arduino, IC LM358N as an op-amp, capacitor, and resistor. IC LM358N was used as a transimpedance amplifier to convert current to voltage and amplify the output voltage of the photodiode. A capacitor was also used in this amplifier to reduce noise. The output voltage represented the light intensity entering the photodiode. The Arduino read the output voltage.

2.3. Data Acquisition

The optical e-nose depends on light interaction with VOCs. The first step was conducting the system calibration for the situation without gases and with carbon dioxide (CO_2) inside the sensor chamber. These measurements were done twice. The resulted data was used as the reference.

The acquisition was divided into three stages, flushing, collection and purging. First, the data was flushed in through a hose from the sample chamber into the sensor or interaction chamber. This stage took place in two minutes. Second, the led was turned on, output voltage data was collected directly by triggering PLX-DAQ. This stage happened in 3 – 5 minutes. Third, the LED was turned off and the gases were purged. However, the data acquisition still took place until the value went to zero. This acquisition process was conducted two times for each sample.

The light intensity was detected in the photodiode and converted to current and to voltage. This voltage was recorded directly using software PLX-DAQ in Microsoft excel, automatically in real-time. Each time the gases interacted with LED light, the Arduino triggered the software to record the data in real-time. The output data were used for analysis to learn a pattern of the ripeness levels of the oil palm fruit.

2.4. Data Analysis

The data to be analyzed consists of the time response of photodiode voltages and trapezoidal area for each sample. Sensor response data is in the form of output voltage curve versus time. Trapezoidal areas were calculated for each sample and wavelength to represent the area under the voltage curve. They were used to see the pattern of each sensor to sample. Interaction of light with VOCs of oil palm fruits were represented by Lambert Beer equation as given by Equation (1) [29]. Equation (2) was used to calculate the trapezoidal area of the time-varying voltage curve [30].

$$I_1 = I_0 \, exp(-\alpha d) \tag{1}$$

The trapezoidal integration method algorithm as the following:

$$L = \frac{h}{2}\left[f(x_0) + 2 \sum_{i=0}^{n-1} f(x_i) + f(x_n) \right] \tag{2}$$

In Equation (1), I_0 is the initial intensity, I_1 is the final intensity after the gas injected into chamber, αd is the constant. This value described the thickness of object in the chamber during measurement. In Equation (2), the value used was the data acquired during measurement. So, the lower limit ($f(x_i)$ and $f(x_n)$) is the minimum value of the data and the higher limit ($f(x_n)$ and h) is the maximum value.

3. RESULTS AND DISCUSSIONS

This research aimed to study the interaction of LED light with VOCs gases emitted by oil palm FFBs fruits. The analysis was based on the time-varying output voltages, trapezoidal area, and the LED wavelengths. The resulting interactions show different patterns for each sample based on the ripeness levels.

3.1. Calibration Results

Figure 3 shows the calibration results using CO_2 and without gases inside the sensor chamber. The calibration without gases shows no absorption curves, which means no interaction occurred. Meanwhile, the calibration using CO_2 shows significant results that there are some absorption curves. This case also indicated that some light with the 760 nm wavelength was absorbed the most by CO_2 gas. The second higher absorbance was LED light at the 910 nm wavelength, followed by 780 nm and 840 nm wavelengths.
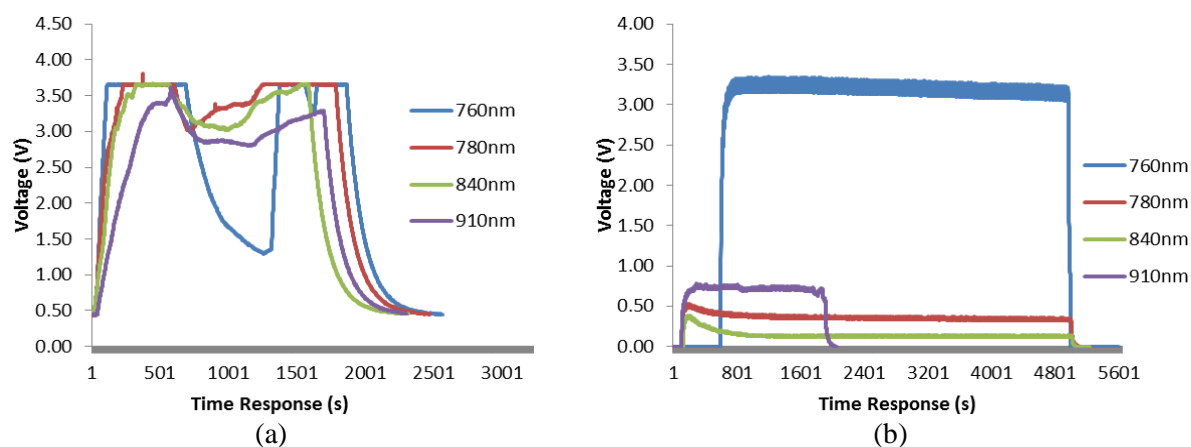

(a)   (b)

Figure 3. Calibration for (a) CO_2 and (b) without gases.

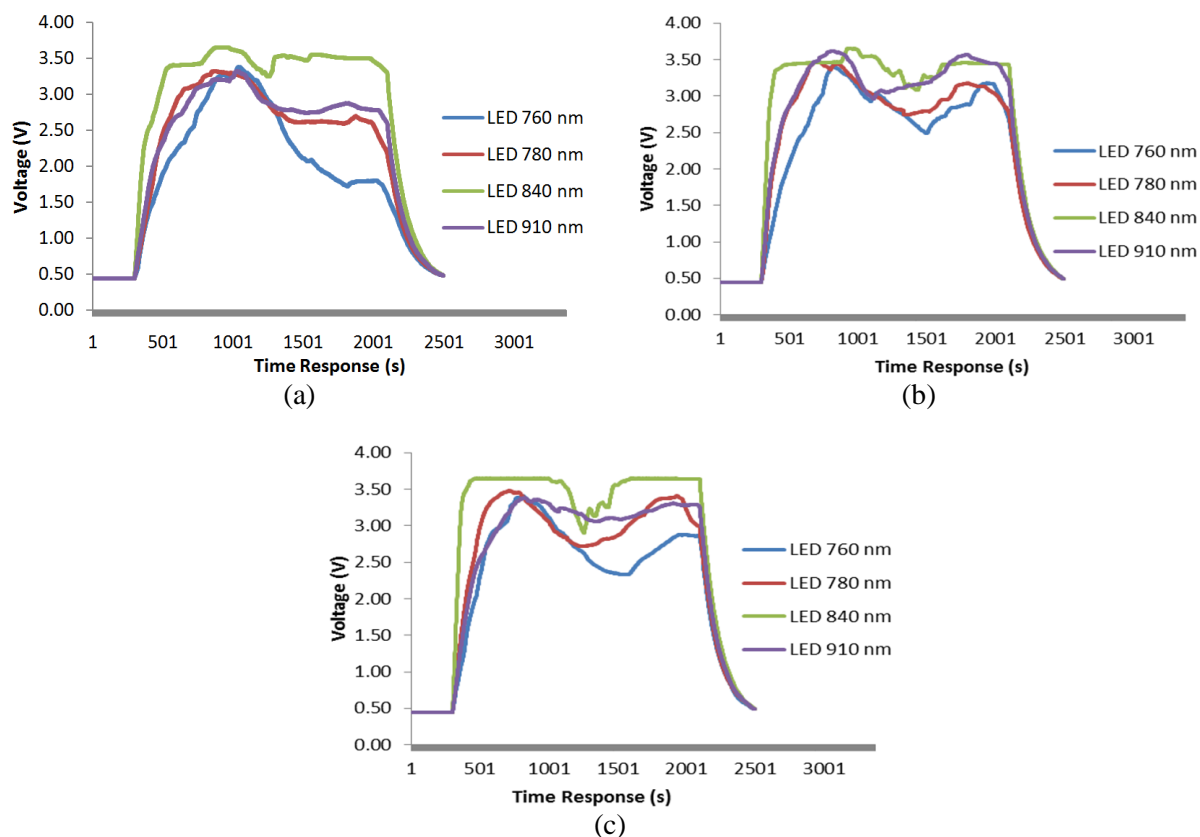(a)   (b)

(c)

Figure 4. Output voltage for each ripeness level (a) unripe, (b) ripe, and (c) overripe.

3.2. Detection Response Time

Figure 4 shows interaction between gases and wavelength. Generally, the curve peak for each ripeness level is different especially for the low peak. The unripe level which is showed in Figure 4 (a) has lower peak than ripe. This indicated that the wavelength was absorbed during interaction. It was slightly different with ripe and unripe level which has peak value is a bit higher that overripe level.

There are 4 wavelengths occupied on this research. The wavelength 760 nm showed a significant reaction to interaction between wavelength and odor for unripe, ripe, and unripe level. The value generated has lower peak than 780, 840, and 910 nm. This case also showed that 760 nm is more sensitive in reading the interaction process.

3.3. Wavelength Dependence of Ripeness Detection

Figure 5 shows different area below of each curve. The value for each maturity level is different. The different area can be seen thatthe unripe level has higher peak area than ripe and overripelevel for wavelength 840 nm but lower for 760, 780, and 910 nm. The ripe level area shows the lower value on the wavelength 840 nm. But there was no lower value shown for the overripe level area.
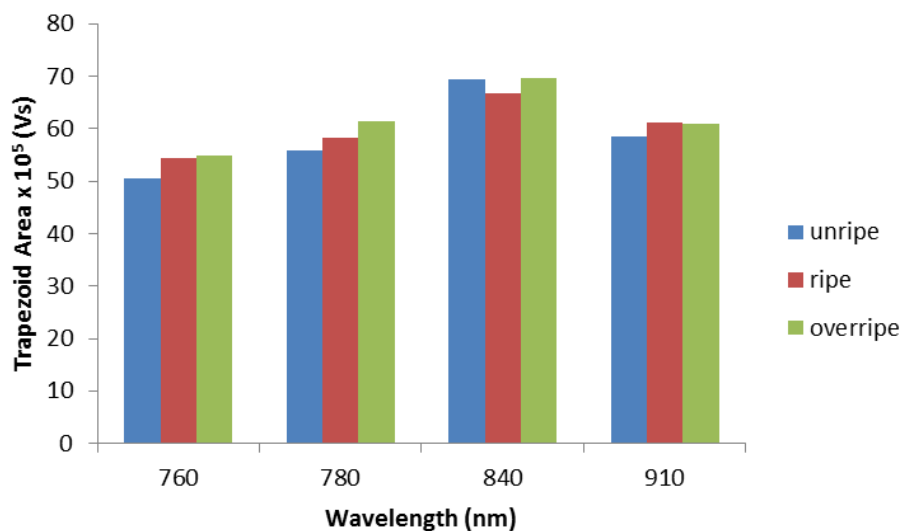

Figure 5. Trapezoid area for each ripeness level.

Beside that, Figure 5 shows a difference value for each level area. The wavelength for 760 nm and 780 nm have the difference value for the trapezoid area. These value shows that 760 nm and 780nm are more sensitive to conduct data acquisition.

4. CONCLUSION

Based on the research with 4 wavelengths that has showed a good response in identifying the level of maturity. The wavelength for 760 nm and 780 nm showed a good and sensitive result in interaction process. This shows that optical enose has the potential to study the characteristics of oil palm fruit. The wavelength and gas reactions also show the patterned behavior so that can distinguish the maturity level of oil palms.

ACKNOWLEDGMENTS

REFERENCES

[1]   L. Cheng, *et al.*, "Development of compact electronic noses: A review," *Measurement Science and Technology*, vol. 32, 062002, Apr 2021.

[2]   M. Mohd Ali, *et al.*, "Principles and recent advances in electronic nose for quality inspection of

agricultural and food products," *Trends in Food Science and Technology*, vol. 99, pp. 1-10, May 2020.

[3] E. Bonah, *et al.*, "Application of electronic nose as a non-invasive technique for odor fingerprinting and detection of bacterial foodborne pathogens: A review," *Journal of Food Science and Technology*, vol. 57, pp. 1977-1990, Nov 2020.

[4] M. Falasconi, *et al.*, "Electronic Nose for Microbiological Quality Control of Food Products," *International Journal of Electrochemistry*, vol. 2012, pp, 1-12, Feb 2012.

[5] W. Jia, *et al.*, "Advances in Electronic Nose Development for Application to Agricultural Products," *Food Analytical Methods*, vol. 12, pp. 2226-2240, Jul 2019.

[6] L. Huang, *et al.*, "A primary study on forecasting the days before decay of peach fruit using near-infrared spectroscopy and electronic nose techniques," *Postharvest Biology and Technology*, vol. 133, pp. 104-122, Jul 2017,

[7] A. D. Wilson and M. Baietto, "Advances in electronic-nose technologies developed for biomedical applications," *Sensors*, vol. 11, pp. 1105–1176, Jan 2011.

[8] A. D. Wilson, "Review of Electronic-nose Technologies and Algorithms to Detect Hazardous Chemicals in the Environment," *Procedia Technology*, vol. 1, pp. 453-463, May 2012.

[9] S. Deshmukh, *et al.*, "Application of electronic nose for industrial odors and gaseous emissions measurement and monitoring - An overview," *Talanta*, vol. 144, pp. 329-340, Nov 2015.

[10] M. Mansurova, *et al.*, "A breath of information: the volatilome," *Current Genetics*, vol. 64, pp. 959-964, Aug 2018.

[11] W. C. Wen, T. I. Chou, and K. T. Tang, "A Gas Mixture Prediction Model Based on the Dynamic Response of a Metal-Oxide Sensor," *Micromachines*, vol. 10, 598, Sep 2019.

[12] X. Liu, *et al.*, "A survey on gas sensing technology," *Sensors*, vol. 12, pp. 9635-9665, Jul 2012.

[13] G. Korotcenkov, "Handbook of Gas Sensor Materials: Properties, Advantages and Shortcomins for Applications," *Springer Science & Business Media*, vol. 1, Jan 2013.

[14] S. Esfahani, *et al.*, "Development of a tuneable NDIR optical electronic nose," *Sensors*, vol. 20, pp. 1-16, Dec 2020.

[15] S. Xu, *et al.*, "Visible/near Infrared Reflection Spectrometer and Electronic Nose Data Fusion as an Accuracy Improvement Method for *Port*able Total Soluble Solid Content Detection of Orange," *Applied Science.* vol. 9, 3761, Sep 2019.

[16] A. T. S. Semeano, *et al.*, "Tilapia fish microbial spoilage monitored by a single optical gas sensor," *Food Control*, vol. 89, pp. 72-76, Feb 2018,

[17] D. J. Murphy, "The future of oil palm as a major global crop: opportunities and challenges," *Journal of Oil Palm Research*, vol. 26, pp. 1-24, Mar 2014.

[18] N. Fadilah, *et al.*, "Intelligent color vision system for ripeness classification of oil palm fresh fruit bunch," *Sensors*, vol. 12, pp. 14179-14195, Oct 2012.

[19] S. Zolfagharnassab, A. R. Mohamed Shariff, and R. Ehsani, "Emissivity determination of oil palm fresh fruit ripeness using a thermal imaging technique," *Acta horticulturae*, vol. 1152, pp. 189-194, Mar 2017.

[20] S. L. Utom, *et al.*, "Non-Destructive Oil Palm Fresh Fruit Bunch (FFB) grading technique using optical sensor," *International Journal of Integrated Engineering*, vol. 10, pp. 35-39, Apr 2018.

[21] N. Sari, *et al.*, "Ripeness Classification of Oil Palm Fresh Fruit Bunch Using an Optical Probe," *Journal of Aceh Physics Society*, vol. 8, pp. 72-77, Sep 2019.

[22] A. H. Abdullah, *et al.*, "Application Specific Electronic Nose (ASEN) for Ganodermaboninense detection using artificial neural network," *2014 2nd International Conference on Electronic Design (ICED)*, pp. 148-152, Aug 2014.

[23] I. Kresnawaty, *et al.*, "Electronic nose for early detection of basal stem rot caused by Ganoderma in oil palm," *IOP Conference Series: Earth and Environmental Science*, vol. 468, 012029, Mar 2022.

[24] M. Shiddiq, *et al.*, "Electronic nose based on mos gas sensor to characterize ripeness of oil palm fresh fruits," *Jurnal Teknik Pertanian Lampung*, vol. 10, pp. 170-182, Jun 2021.

[25] M. Baietto and A. D. Wilson, "Electronic-nose applications for fruit identification, ripeness and quality grading," *Sensors*, vol.15, pp. 899-931, Jan 2015.

[26] M. Koushki, M. Nahidi, and F. Cheraghali, "Physico-chemical properties, fatty acid profile and nutrition in palm oil," *Journal of paramedical sciences*, vol. 6, pp. 117-134, Aug 2015.

[27] A. H. J. Kuntom, P. J. Dirinck, and N. M. Schamp, "Identification of volatile compounds that contribute to the aroma of fresh palm oil and oxidized oil," *Journal of Oil Palm Research*, vol. 1, pp. 53-61, Jun 1989.

[28] N. H. Harun, *et al.*, "Investigations on a Novel Inductive Concept Frequency Technique for the grading of Oil Palm Fresh Fruit Bunches," *Sensors*, vol. 13, pp. 2254-2266, Feb 2013.

[29] M. Volterrani, *et al.*, "Reflectance, absorbance and transmittance spectra of bermudagrass and manilagrassturfgrass canopies," *PLoS ONE*, vo. 12, pp. 1-13, Nov. 2017.

[30] M. Harker and P. O'Leary, "Trapezoidal rule and its error analysis for the Grünwald-Letnikov operator," *International Journal of Dynamics and Control*, vol. 5, pp. 18-29, Mar 2017.